

FIG. 1. (a) Atomic structure of fully relaxed bare armchair Si nanoribbon of width $n = 9$ (ASiNR-9). (b) Atomic structure and bond length distribution of hydrogen saturated ASiNR-9. Similar pattern is observed in hydrogen saturated AGeNR-9. The primitive unit cell of ASiNR-9 is shaded. The zigzag chain of Si atoms perpendicular to the nanoribbon axis is delineated by the dashed lines.

pling parameters of empirical tight binding calculations are determined from the *ab initio* results and are used to treat wide and long superlattice structures, comprising as many as 3600 Si atoms.

III. ATOMIC STRUCTURE AND STABILITY

We first investigate the atomic structure of bare and hydrogen saturated armchair nanoribbons of Si and Ge. The ideal honeycomb structure is cut parallel to the nearest neighbor bonds to form an ideal bare nanoribbon with a certain width. Armchair nanoribbons are classified by counting the number, n , of Si (or Ge) atoms forming a zigzag chain perpendicular to the cut direction. Accordingly, there are $2n$ Si (or Ge) atoms in the primitive unit cell of an ideal bare armchair nanoribbon. This structure is treated by a supercell having periodic boundary condition in cut direction and a vacuum spacing in other directions. To lift the constraints imposed by (1×1) unit cell, we have used (2×1) supercell. Figure 1(a) presents the atomic structure of a sample bare armchair Si nanoribbon after structural relaxation. Here one can see a (2×1) reconstruction at the edges, which would be missed if (1×1) unit cell was used in the calculation. The edge reconstruction is reminiscent of the reconstruction of Si(100)- (2×1) surface. In the latter case, two adjacent surface Si atoms each having two sp^3 -dangling bonds come closer and form a new dimer bond using one sp^3 -dangling bond from each atom. At the end, the number of sp^3 dangling bonds is halved and hence the energy is lowered through reconstruction. Similarly, in Fig.1(a) A and B atoms come closer to form a bond. Since the nature of bonding is modified around B atom, the ABC triangle is bowed. At the end, the number of the sp^2 dangling bonds is halved. Note that, this kind of reconstruction is

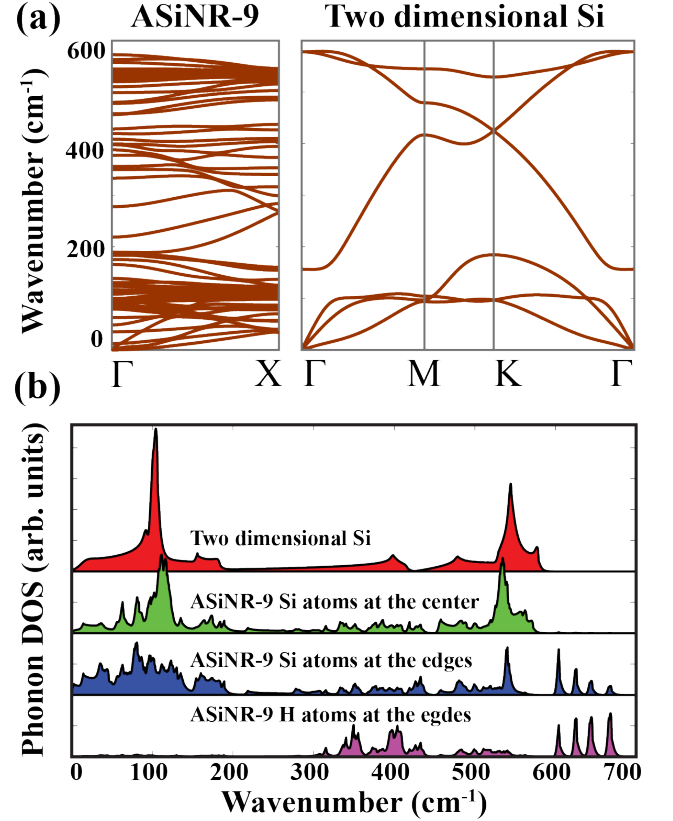


FIG. 2. (a) Phonon dispersions calculated for hydrogen saturated ASiNR-9 and for 2D honeycomb structure of Si. States that appear above 600 cm^{-1} are related to Si-H bonds of hydrogen saturated ASiNR-9 and were not shown. (b) Phonon densities of states (DOS) of the hydrogen saturated ASiNR-9 projected to Si atoms at the center and at the edges and also to H atoms at the edges. DOS of 2D honeycomb structure of Si is also presented for comparison.

not seen in bare armchair graphene nanoribbons. Moreover, in graphene and its nanoribbons all atoms lie in the same plane, while structures considered here are slightly buckled. The separation between adjacent atoms in the perpendicular direction to the plane is around 0.4 \AA and 0.6 \AA for Si and Ge nanoribbons, respectively.

Figure 1(b) presents the atomic structure and bond length distribution of a sample hydrogen saturated armchair silicon nanoribbons. In contrast to bare nanoribbons, saturation by hydrogen lifts the (2×1) reconstruction at the edges. In Fig. 1(b) there are $n = 9$ Si atoms forming zigzag chain perpendicular to the nanoribbon axis and hence this armchair nanoribbon is classified as ASiNR-9. Accordingly the number of Si (or Ge) atoms in the primitive unit cell is $2n$. Note that the bond length distribution is nearly uniform except a sudden decrease at the edges. This pattern was also observed in armchair graphene nanoribbons.²⁰

Figure 2(a) presents the phonon dispersion profile for hydrogen saturated ASiNR-9. Also phonon dispersion profile of 2D silicon, reproduced from Ref. [14], was